Peptides 35 (2012) 86–94

Contents lists available at SciVerse ScienceDirect

Peptides

journal homepage: www.elsevier.com/locate/peptides

Larazotide acetate regulates epithelial tight junctions in vitro and in vivo

Shobha Gopalakrishnan[a], Malarvizhi Durai[a], Kelly Kitchens[a,1], Amir P. Tamiz[a], Robert Somerville[a,2], Mark Ginski[a,3], Blake M. Paterson[a,4], Joseph A. Murray[b], Elena F. Verdu[c], Sefik S. Alkan[a,5], Niranjan B. Pandey[a,*]

[a] ALBA Therapeutics, 650 S. Exeter, Suite 1040, 10th Floor, Baltimore, MD 21202, United States
[b] Mayo Clinic, Department of Medicine and Immunology, 200 First Street SW, Rochester, MN 55905, United States
[c] Department of Medicine, McMaster University, HSC-3N5C, L8N3Z5, Canada

ARTICLE INFO

Article history:
Received 13 December 2011
Received in revised form 20 February 2012
Accepted 20 February 2012
Available online 27 February 2012

Keywords:
Celiac disease
Gliadin
ZO-1
Actin
Tight junction
Permeability inducer

ABSTRACT

Tight junctions (TJs) control paracellular permeability and apical-basolateral polarity of epithelial cells, and can be regulated by exogenous and endogenous stimuli. Dysregulated permeability is associated with pathological conditions, such as celiac disease and inflammatory bowel disease. Herein we studied the mechanism by which larazotide acetate, an 8-mer peptide and TJ regulator, inhibits the cellular changes elicited by gliadin fragments, AT-1002, and cytokines. Previously, we demonstrated that AT-1002, a 6-mer peptide derived from the *Vibrio cholerae* zonula occludens toxin ZOT, caused several biochemical changes in IEC6 and Caco-2 cells resulting in decreased transepithelial electrical resistance (TEER) and increased TJ permeability. In this study, larazotide acetate inhibited the redistribution and rearrangement of zonula occludens-1 (ZO-1) and actin caused by AT-1002 and gliadin fragments in Caco-2 and IEC6 cells. Functionally, larazotide acetate inhibited the AT-1002-induced TEER reduction and TJ opening in Caco-2 cells. Additionally, larazotide acetate inhibited the translocation of a gliadin 13-mer peptide, which has been implicated in celiac disease, across Caco-2 cell monolayers. Further, apically applied larazotide acetate inhibited the increase in TJ permeability elicited by basolaterally applied cytokines. Finally, when tested in vivo in gliadin-sensitized HLA-HCD4/DQ8 double transgenic mice, larazotide acetate inhibited gliadin-induced macrophage accumulation in the intestine and preserved normal TJ structure. Taken together, our data suggest that larazotide acetate inhibits changes elicited by AT-1002, gliadin, and cytokines in epithelial cells and preserves TJ structure and function in vitro and in vivo.

1. Introduction

Multicellular organisms can survive only if they establish a distinct internal environment, separating "self" from the "non-self" environment. The mucosal surfaces of the genitourinary, gastrointestinal, and respiratory tracts have epithelial barriers that are "sealed" by tight junctions (TJs) [31,40]. TJs are located at the apicolateral borders of adjoining epithelial cells, regulating the patency of the paracellular space and limiting the bidirectional diffusion of particles, water, and solutes across mucosal surfaces. TJs consist of over 50 proteins, including the transmembrane proteins junctional adhesion molecule (JAM), occludin, and claudin, and the cytoplasmic scaffolding proteins zonula occludens (ZO)-1, ZO-2, and ZO-3 [1,16].

In the absence of inflammation or epithelial disruption, the functional state of the TJ determines paracellular permeability and polarity [33]. TJs are highly dynamic, opening and closing in response to cytoskeletal reorganization that occurs upon exposure to external antigens, such as gliadin in celiac disease [30], and internal inflammatory cytokines, such as TNF-α [31]. Increased exposure

Abbreviations: TJ, tight junction; TEER, transepithelial electrical resistance; LY, lucifer yellow; AT-1002, permeability inducer, 6-mer peptide; AT-1001, tight junction regulator, 8-mer peptide (larazotide acetate).

* Corresponding author. Present address: 720 Rutland Ave., 617 Traylor Bldg., Systems Biology Laboratory, Department of Biomedical Engineering, School of Medicine, Johns Hopkins University, Baltimore, MD 21205, United States. Tel.: +1 410 614 2951; fax: +1 410 614 8796.
E-mail address: pandey.niranjan@gmail.com (N.B. Pandey).
[1] Present address: MPN1, Rockville, MD 20855, United States.
[2] Present address: National Cancer Institute, Surgery Branch, Building 10 CRC, Room 3-3825, 9000 Rockville Pike, Bethesda, MD 20892, United States.
[3] Present address: 5217 Scenic Drive, Perry Hall, MD 21128, United States.
[4] Present address: Department of Anesthesia and Critical Care Medicine, Johns Hopkins University School of Medicine, 600 N. Wolfe Street, Meyer 8-140, Baltimore, MD 21287, United States.
[5] Present address: Alkan Consulting LLC, Mittlere Strasse 8, CH-4056 Basel, Switzerland.

0196-9781/$ – see front matter © 2012 Elsevier Inc. All rights reserved.
doi:10.1016/j.peptides.2012.02.015

of the submucosa to external antigens is putatively caused by "barrier dysfunction" in the small bowel, and "intestinal leak" is associated with numerous intestinal and extra-intestinal autoimmune conditions, including celiac disease, inflammatory bowel disease, type 1 diabetes, multiple sclerosis, primary biliary cirrhosis, autoimmune hepatitis, and systemic sclerosis [14,15,42].

Celiac disease, an autoimmune disorder, is triggered by gluten/gliadin or gliadin fragments in individuals with the HLA-DQ2/DQ8 allele that facilitates presentation of gliadin peptides to T cells [20]. Gliadin induces a loss of barrier function and stimulates innate and adaptive immune responses, followed by intestinal damage [29]. Gliadin also disrupts TJ integrity by altering actin and ZO-1 distribution in intestinal epithelial cells [9,12,30]. Alterations in ZO-1 phosphorylation and expression have also been reported in response to gliadin and in celiac disease mucosa, respectively [7,30].

Protease-resistant gliadin peptides are transported, by as yet unknown mechanisms, from the lumen of the gut to the lamina propria, where tissue transglutaminase catalyzes the conversion of glutamine in certain peptides to glutamate. Deamidated versions of the gliadin peptides cause immune activation and initiate an inflammatory cascade with the production of IFNγ and other cytokines [17]. One of the "toxic" gliadin peptides, P31–43 (13-mer), also induces intestinal permeability and stimulates cytokine and chemokine production by macrophages in vitro [39]. Inflammatory cytokines have been shown to enhance the permeability of the gut epithelium [2,8], which could lead to the translocation of more gliadin. Currently, a gluten-free diet is the only management that helps to alleviate the symptoms of celiac disease [10]. Therefore, there is a great need for novel therapeutic approaches that target the earliest event at the mucosal surface to inhibit barrier dysfunction, and hence prevent immune activation.

We have previously shown that AT-1002, a synthetic peptide comprising the first 6 amino acids of the active fragment of zonula occludens toxin (ZOT) from *Vibrio cholerae*, lowers transepithelial electrical resistance (TEER) and increases TJ permeability and alters ZO-1 and actin distribution in Caco-2 cells [19]. As mentioned previously, gliadin also elicits similar responses in intestinal epithelial cells. It is also well established that cytokines decrease TEER and induce paracellular permeability in epithelial cells [32,45]. We have developed an 8-mer peptide and TJ regulator larazotide acetate that has therapeutic value for celiac disease owing to its ability to inhibit early mucosal events that lead to barrier dysfunction and immune activation [26]. Furthermore, ZOT-induced immune responses are inhibited by intranasal administration of larazotide acetate [22], and oral larazotide acetate reduces the incidence of type I diabetes in BB Wor/DP rats [46]. In this study, we examined the mechanism by which larazotide acetate inhibits TJ opening caused by AT-1002, gliadin, and cytokines. We studied effects on TJ and cytoskeletal organization in vitro, and examined whether the "epithelial leak" induced by various stimuli was inhibited by larazotide acetate. Finally, we examined whether these in vitro effects of larazotide acetate on TJs could be translated in vivo to a gluten-sensitive transgenic HLA-HCD4/DQ8 mouse model developed at the Mayo clinic [5]. In this mouse model, gluten sensitization induces changes in intestinal permeability and innate immune cell infiltration making it an excellent model to test potential therapeutics for gluten-induced effects [25,28].

2. Materials and methods

2.1. Reagents

The permeability inducer AT-1002 and the 13-mer gliadin peptide AT-4067 were synthesized using F-moc solid phase chemistry as described previously [19]. The final products were isolated as TFA salts in a lyophilized form (>95% purity by HPLC/MS).

Larazotide acetate (AT-1001) was synthesized using solution phase synthesis [9], and the identity of the compound was confirmed by LC/MS. The final product was isolated as an acetate salt in a lyophilized form (>99% purity by HPLC/MS).

Pepsin-trypsin treated gliadin (PTG) was prepared as described previously [39]. Recombinant interleukin (rIL)-1β, interferon (IFN)-γ, and tumor necrosis factor-α (rTNF-α) were purchased from R&D Systems (Minneapolis, MN).

2.2. Cell lines

Caco-2 BBE (brush border-expressing) cells were obtained from American Type Culture Collection (ATCC, Manassas, VA) and maintained in Dulbecco's Modified eagle Medium (DMEM; Invitrogen, Carlsbad, CA) containing 10% fetal bovine serum, penicillin (100 units/mL), streptomycin (100 μg/mL), and 100 μg/mL human transferrin. Cells were plated at 100,000 cells per 12-well filter and used at 10–14 days post-seeding.

Caco-2 cells were obtained from ATCC and maintained in DMEM containing 10% fetal bovine serum, penicillin (100 units/mL), and streptomycin (100 μg/mL).

IEC6 cells were obtained from ATCC and maintained in DMEM containing 0.1 unit/mL bovine insulin, 10% fetal bovine serum, penicillin (100 units/mL), and streptomycin (100 μg/mL). Cells were seeded on 8-chamber slides at 60,000 cells per chamber for immunofluorescence studies.

IEC6 cells were used to study gliadin effects because Caco-2 cells did not respond to gliadin in our hands. Although IEC6 cells formed TJs and expressed ZO-1 at cell-cell junctions, their baseline permeability was quite high. Therefore, these cells were used mainly for ZO-1 imaging studies and not for functional assays.

2.3. Lucifer yellow (LY) permeability assays

Details of this method and modifications have been described previously [4,18]. Briefly, Caco-2 cells were seeded onto 12-well Transwells™ and grown for 21–28 days until fully differentiated. The apical and basolateral compartments of Caco-2 cell monolayers were pre-incubated in Hank's Balanced Salt Solution (HBSS) at 37 °C for 30 min. Treatment solutions containing 7.5 mM LY with or without AT-1002 (7 mM) and different concentrations of larazotide acetate in HBSS were added to the apical compartment of each monolayer and incubated at 37 °C, 50 rpm for 180 min. At the end of the incubation, samples were removed from the basolateral compartment and analyzed in a Tecan Spectrofluor fluorescence plate reader at excitation and emission wavelengths of 485 nm and 535 nm, respectively. The increase in LY passage was calculated for each treatment and is expressed relative to that of untreated controls.

2.4. Immunofluorescence

Cells were washed in serum-free medium and incubated with 12.5 mM larazotide acetate diluted in serum-free medium for 30 min at 37 °C. Larazotide acetate was removed and cells were incubated with PTG (2.5 mg/mL) or AT-1002 (7 mM) in the presence or absence of larazotide acetate (12.5 mM) at 37 °C for 60 min or 180 min, respectively. Following treatment, cells were washed in PBS and fixed in 4% paraformaldehyde for 15 min at room temperature, or in ice-cold methanol:acetone (1:1) for 7 min. Cells were washed in PBS, permeabilized in PBS containing 0.5% Triton X-100 for 5 min at room temperature (for paraformaldehyde fixed cells), and blocked in PBS containing 2% goat serum for 30 min at room temperature. Actin and ZO-1 were detected using Alexa

Fluor555-phalloidin (1:20) and FITC-conjugated anti-ZO-1 antibody (1:200; Invitrogen), respectively. Slides were washed and mounted in Vectashield containing DAPI. Images were collected on a Nikon-TE2000 fluorescence microscope using a 40× objective and quantified using Adobe Photoshop, as described previously [19]. Briefly, the background level was adjusted using the threshold function. Then the brightness was adjusted to bring all background pixels to the threshold value. Pixels at cell-cell junctions were highlighted using the Magic wand and select/inverse functions. The mean pixel intensity value, total number of pixels, and number of threshold pixels were obtained. Total junctional fluorescence intensity = (total pixels × mean pixel value) − (threshold pixels × threshold) was calculated for each sample. A total of 40 cells were quantified per treatment per experiment. The settings were kept the same for all groups. Two independent experiments were performed. Data are expressed as mean (SD), and a p value of <0.05 was considered significant.

2.5. F-actin flow cytometry

Caco-2 BBE cells were treated apically with AT-1002 (7 mM) in the presence or absence of larazotide acetate (12.5 mM) for 3 h at 37 °C. Following treatment, cells were detached from filters using trypsin. Detached cells were washed in PBS, fixed in PBS containing 4% paraformaldehyde for 15 min at room temperature, permeabilized in PBS containing 0.5% Triton X-100 for 5 min at room temperature, and blocked in PBS containing 2% goat serum for 30 min at room temperature. Cells were incubated with Alexa Fluor555-phalloidin for 1 h at room temperature, washed in PBS, and 10,000 cells from each sample were analyzed by flow cytometry using FACSCAN (Becton Dickinson, San Diego, CA).

2.6. Gliadin peptide translocation

Caco-2 cells were seeded at 100,000 cells/cm^2 on 12-well Transwell® filters. At 21–28 days post-seeding, cells were treated with FITC-labeled gliadin 13-mer fragment (AT-4067; 1 mM) in the presence or absence of larazotide acetate (100 μM) for 3 h at 37 °C, 95% relative humidity, 50 rpm, and 5% CO_2. At t = 3 h, samples were removed from the receiver compartment and analyzed in a Tecan Spectrofluor fluorescence plate reader at excitation and emission wavelengths of 485 nm and 535 nm, respectively. Gliadin permeability was calculated for each treatment and expressed relative to untreated control conditions.

2.7. Cytokine treatment and permeability assay

Caco-2 cells were seeded at 60,000 cells/cm^2 in 24-well Transwell® plates, and maintained in culture medium composed of Dulbecco's Modified Eagle's Medium, 10% fetal bovine serum, 1% non-essential amino acids, and 2% penicillin-streptomycin. Medium was changed twice a week with 0.2 mL and 1.0 mL for apical and basolateral sides, respectively. Assays were performed 21–24 days post-seeding. On the day of the experiment, Caco-2 cells were incubated in complete RPMI (RPMI 1640 media containing 1% penicillin-streptomycin, 1% HEPES, 1% sodium pyruvate, 1.8 μL of 2-mercaptoethanol, and 5% human AB serum) for 2 h at 37 °C, in 5% CO_2. After incubation, Caco-2 cells were treated basolaterally with 1 mL of complete RPMI containing 50 ng/mL each of TNF-α, IFNγ, and IL-1β (R&D Systems) for 72 h at 37 °C in 5% CO_2. For larazotide acetate treatment, medium was replaced with different doses of larazotide acetate on the apical side after 48 h. At the end of the experiment, LY flux was measured as follows: medium was replaced with LY (7.5 mM) on the apical side and cells were incubated for 1 h at 37 °C, 50 rpm. Samples (100 μL) were collected from the basolateral side and the amount of LY was quantified by measuring fluorescence at excitation and emission wavelengths of 485 nm and 535 nm, respectively.

2.8. Treatment of HLA-HCD4/DQ8 mice with larazotide acetate

Cohorts of HLA-HCD4/DQ8 mice (n = 10 each) were sensitized (i.p.) with 500 μg of gliadin (Sigma-Aldrich, Oakville, Ontario, Canada) dissolved in 0.02 mM acetic acid in 50 μg of Complete Freund's Adjuvant (CFA; Sigma-Aldrich); thereafter, mice were gavaged with gliadin (2 mg/mouse), +/− treatment, 2×/week for 7 weeks. Group 1 received larazotide acetate (250 μg/mouse) and gliadin, Group 2 received AT-1002 (250 μg/mouse) and gliadin, and Group 3 was gavaged with gliadin only. A group of non-sensitized controls (CFA, i.p. only) was gavaged with rice. Twenty-four hours after the last gavage, small intestinal tissue was mounted in Ussing chambers for the measurement of electrical parameters (*Isc*, conductance) and macromolecule transport (horseradish peroxidase [HRP] flux). Tissue was processed for macrophage counts by immunohistochemistry using F4/80 antibody specific for a macrophage-restricted cell surface glycoprotein.

2.9. Immunohistochemistry for macrophages

Jejunal sections obtained from HLA-HCD4/DQ8 mice were immunostained for macrophages using a technique previously described [44]. Briefly, immunostaining was performed on paraffin sections using a monoclonal antibody specific for the F4/80 antigen. The rat anti-mouse F4/80 antibody (1:200; Serotec, Oxford, UK) was followed by biotinylated polyclonal goat anti-rat antibody (1:200; Cederlane Laboratories, Hornby, BC, Canada) and then streptavidin/horseradish peroxidase (1:300; Dakocytomation). Antibodies were visualized by diaminobenzidine and counterstaining with Mayer's hematoxylin. Negative controls were performed in the absence of primary antibody. F4/80-positive cells were quantified in 5 villi, in 2 different sections per mouse (averaged). Data were analyzed using two-way ANOVA, and expressed as mean (SD). A p value <0.05 was considered significant.

2.10. Electron microscope (EM) analysis of TJ

Additional jejunal sections from HLA-HCD4/DQ8 mice were obtained and immediately fixed in 2.5% glutaraldehyde in 0.1 mol/L sodium cacodylate buffer (pH 7.4) for 2 h at room temperature, transferred to sodium cacodylate buffer, and stored at 4 °C overnight. Tissues were washed 3 times in 0.05 mol/L Tris buffer and then incubated for 30 min in 5 mg of 3,3-diaminobenzadine tetrahydrochlorine (Sigma Chemicals, St Louis, MO) in 10 mL of 0.05 mol/L Tris buffer and 0.01% hydrogen peroxide. Tissues were subsequently processed for electron microscopy, and photomicrographs prepared. The fraction of TJ with altered structures was calculated as total open TJ divided by total number of TJ evaluated in 20 fields per mouse in a blinded manner (3–20 tight junctions/field, 60–400 tight junctions/mouse, 4 mice/group). A field is defined as one square in the EM grid, measuring 8100 mm^2. Data were analyzed using two-way ANOVA, and expressed as mean (SD). A p value <0.05 was considered significant.

2.11. Statistics

Data are expressed as mean (SD) or mean (SE), as indicated in the figure legends. Statistical analysis was performed with the t-test or ANOVA using Microsoft Excel. A p-value <0.05 was considered significant.

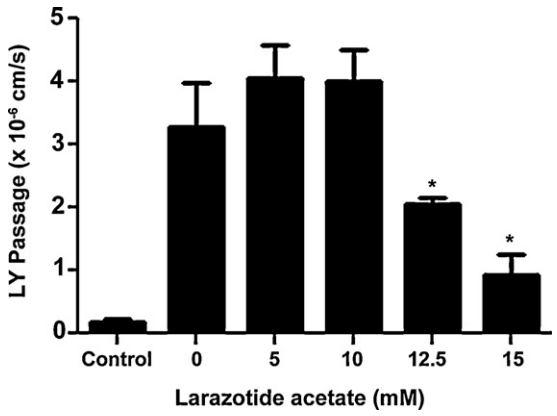

Fig. 1. Larazotide acetate inhibits AT-1002-induced tight junction permeability in Caco-2 cells. (A) Mean permeability of lucifer yellow (LY) across Caco-2 cell monolayers was measured following exposure to AT-1002 in the presence or absence of a series of concentrations of larazotide acetate (LA) ($n = 3$ experiments with 3 wells per group per experiment). Data are expressed as mean (SE). $^*p < 0.05$ vs. AT-1002 alone.

3. Results

3.1. Effects of larazotide acetate on AT-1002-induced TJ dysfunction in Caco-2 cells

We have previously shown that AT-1002 induces TJ barrier dysfunction in human-derived Caco-2 cells [19]. To determine the effects of larazotide acetate on AT-1002-induced barrier dysfunction, we measured the mean LY passage across Caco-2 cell monolayers following exposure to AT-1002 in the presence or absence of larazotide acetate (Fig. 1). AT-1002 caused a substantial increase in LY passage, which was inhibited by larazotide acetate in a dose-dependent manner. Larazotide acetate at 15 and 12.5 mM significantly inhibited the AT-1002-induced increase in LY passage by 71 and 38%, respectively ($p < 0.05$).

3.2. Effects of larazotide acetate on AT-1002-induced ZO-1 redistribution and actin rearrangement in Caco-2 cells

AT-1002 induces the redistribution of ZO-1, an important marker of TJ integrity [19]. We sought to determine whether larazotide acetate inhibited these changes. To this end, Caco-2 BBe cells were treated with AT-1002 in the presence or absence of larazotide acetate, and ZO-1 distribution was examined by immunofluorescence. A z-series of images was collected and projected onto a single plane to avoid missing fluorescence from out-of-focus planes, and ZO-1 junctional fluorescence intensity was quantified. As shown in Fig. 2A, untreated cells and cells treated with larazotide acetate alone exhibited a smooth distribution of ZO-1 at cell-cell junctions. AT-1002 treatment caused extensive redistribution of ZO-1 away from cell junctions, which was inhibited by larazotide acetate. Quantification of total junctional fluorescence intensity revealed that AT-1002 elicited a 60% decrease in junctional ZO-1. However, co-incubation of AT-1002 with larazotide acetate resulted in less than a 10% decrease in junctional distribution of ZO-1 ($p < 0.05$) (Fig. 2A), indicating that larazotide acetate inhibited AT-1002-induced ZO-1 redistribution.

TJ are associated with and stabilized by the cortical actin cytoskeleton, and AT-1002 causes actin rearrangement [19]. To examine the effect of larazotide acetate on AT-1002-induced actin rearrangement, Caco-2 BBe cells were treated with AT-1002 for 1 h in the presence or absence of larazotide acetate, and filamentous actin was visualized by immunofluorescence using fluorescent phalloidin. A z-series of images was acquired and combined into a projection and fluorescence intensity was quantified. Untreated Caco-2 BBE cells exhibited a robust network of actin filaments (Fig. 2B). Exposure to AT-1002 caused dissolution of the actin network, which was prevented by larazotide acetate. Actin fluorescence was quantified by flow cytometry (10,000 cells/sample). AT-1002 decreased the mean F-actin fluorescence intensity to 61% that of control levels, whereas larazotide acetate significantly inhibited the AT-1002-induced loss of F-actin ($p < 0.05$) (Fig. 2B).

3.3. Effects of larazotide acetate on gliadin-induced changes in IEC6 cells

Celiac disease is triggered by gluten/gliadin or gliadin peptides, which disrupt TJ structure and function. Gliadin causes actin rearrangement and ZO-1 redistribution. To determine if larazotide acetate could inhibit the effects of gliadin, rat intestinal epithelial (IEC6) cells were treated with PTG, a source of gliadin fragments generated by digesting gliadin with pepsin and trypsin, diluted in serum-free medium in the presence or absence of larazotide acetate for 1 h, and ZO-1 was visualized by immunofluorescence. In untreated IEC6 cells, ZO-1 exhibited a smooth, uninterrupted distribution at cell-cell junctions; PTG treatment caused a redistribution of ZO-1 away from cell junctions, and junctional fluorescence intensity decreased by 75% (Fig. 3A). PTG-induced ZO-1 redistribution was inhibited by larazotide acetate and the junctional ZO-1 fluorescence intensity was maintained at near control levels (Fig. 3A).

We also examined the effect of larazotide acetate on the actin cytoskeleton in PTG-treated IEC6 cells. PTG caused actin network disassembly; in cells treated with PTG and larazotide acetate, the actin network was protected from disassembly. Furthermore, in the presence of larazotide acetate the junctional distribution of actin appeared more robust. These data suggest that larazotide acetate prevented the PTG-induced disassembly of the actin cytoskeleton (Fig. 3B).

3.4. Effect of larazotide acetate on gliadin translocation

Gliadin peptides are thought to translocate across the epithelial monolayer in the gut [6,35]. We examined whether translocation of the gliadin 13-mer peptide AT-4067 (Leu-Gly-Gln-Gln-Gln-Pro-Phe-Pro-Pro-Gln-Gln-Pro-Tyr) [13,27] could be inhibited by larazotide acetate. Thus, using the Transwell system, FITC-labeled gliadin 13-mer peptide fragment (AT-4067) and larazotide acetate were applied to the apical side of Caco-2 cells at time 0, and the amount of FITC-labeled gliadin 13-mer peptide fragment in the basolateral compartment was measured 3 h later. We found that apically applied larazotide acetate at concentrations as low as 1 mM significantly inhibited translocation of FITC-labeled gliadin 13-mer peptide fragment into the basolateral side ($p < 0.05$) (Fig. 4). We obtained similar results with the FITC-labeled gliadin 9-mer and 33-mer peptides Pro-Phe-Pro-Gln-Pro-Gln-Leu-Pro-Tyr and Leu-Gln-Leu-Gln-Pro-Phe-Pro-Gln-Pro-Gln-Leu-Pro-Tyr-Pro-Gln-Pro-Gln-Leu-Pro-Tyr-Pro-Gln-Pro-Gln-Leu-Pro-Tyr-Pro-Gln-Pro-Gln-Pro-Phe, respectively [36] (data not shown).

3.5. Effect of larazotide acetate on cytokine-induced TJ dysfunction

Gliadin peptides cause immune activation and initiate an inflammatory cascade with the production of IFNγ and other cytokines [20]. It is well established that cytokine treatment reduces TEER and increases paracellular permeability of epithelial cell monolayers [32,45]. We sought to determine whether larazotide acetate could inhibit the cytokine-induced permeability of Caco-2 cells. As shown in Fig. 5, basolateral treatment of Caco-2 cells

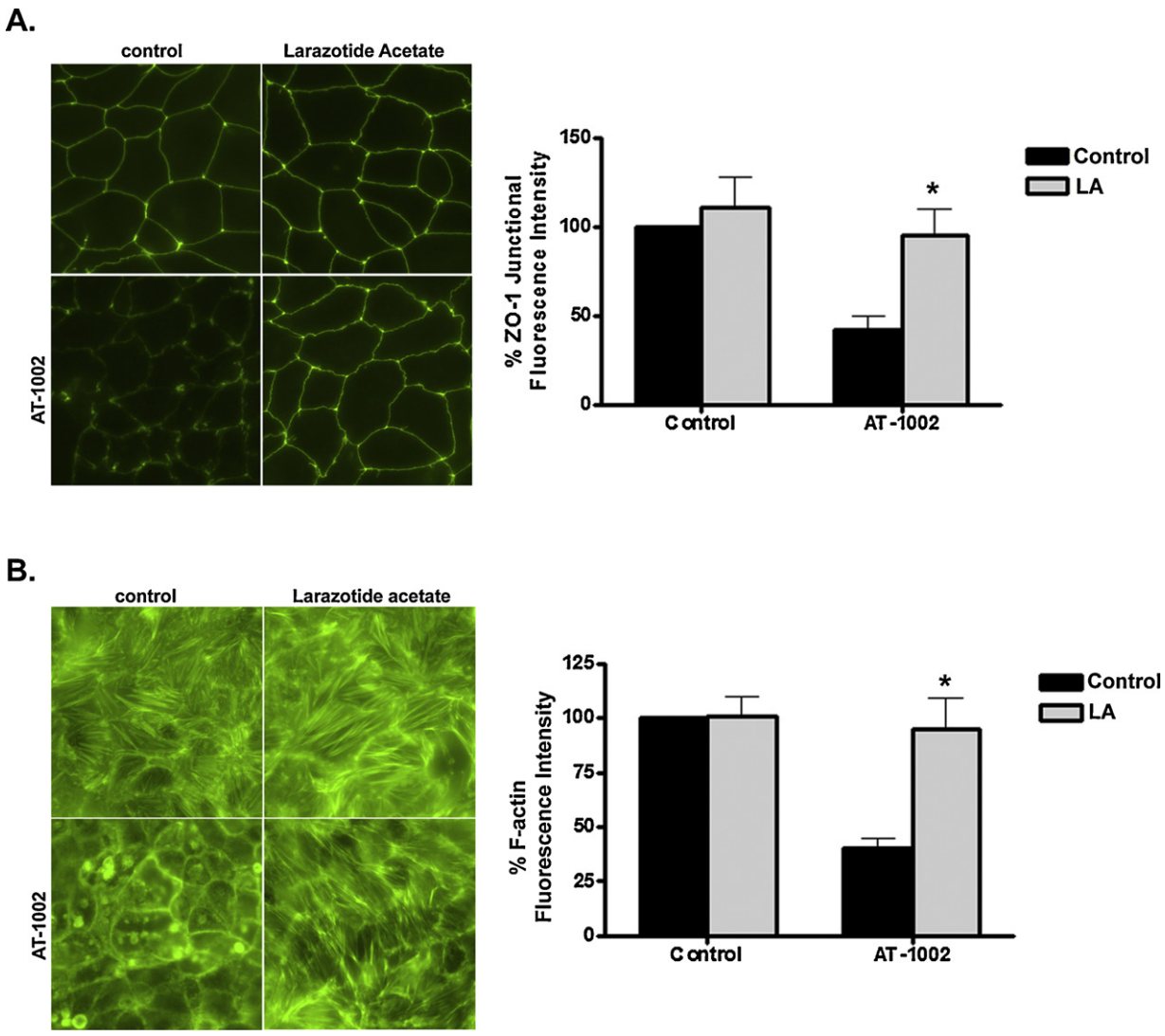

Fig. 2. Larazotide acetate (LA) inhibits AT-1002-induced ZO-1 redistribution and actin rearrangement in Caco-2 cells. Caco-2 BBe cells grown on permeable membrane supports were treated apically with AT-1002 (7 mM) in the presence or absence of larazotide acetate for 3 h at 37 °C. (A) Cells were fixed and processed for immunofluorescence using anti-ZO-1 antibodies. Graph represents percent junctional fluorescence intensity of ZO-1. Data are expressed as mean (SD) and are representative of 3 independent experiments. *$p < 0.05$ vs. AT-1002. (B) Flow cytometric analysis of F-actin fluorescence. Cells were fixed and stained for F-actin using fluorescent phalloidin, and 10,000 cells/sample were analyzed by flow cytometry for actin fluorescence. Data are expressed as mean (SD) and are representative of 4 independent experiments.*$p < 0.05$ vs. AT-1002.

with a mixture of TNF-α, IFN-γ, and IL-1β (50 ng/mL each) caused a substantial increase in permeability, which was significantly inhibited by apically applied larazotide acetate at 3 and 1 mM ($p < 0.05$ vs. cytokine treatment for both) (Fig. 5).

3.6. *In vivo effect of larazotide acetate on intestinal permeability in HLA-HCD4/DQ8 mice*

We tested the effects of larazotide acetate on gliadin-induced alterations in barrier function and macrophage recruitment in double transgenic HLA-HCD4/DQ8 mice [5]. We found that gliadin sensitization and challenge increased conductance (40.1 mS/cm^2) values, which is indicative of a fall in tissue resistance, compared to non-sensitized controls (24.4 mS/cm^2) (Fig. 6A). We also found that gliadin sensitization and challenge increased HRP flux, a measurement of transcellular permeability, from 19.4 (non-sensitized controls) to 86.8 pmol/cm^2/h (Fig. 6B). Larazotide acetate normalized the conductance (26 mS/cm^2) and moderately attenuated the HRP flux (59 pmol/cm^2/h). The improvement in barrier function parameters by larazotide acetate in gliadin sensitized-mice was associated with improved TJ structure, as assessed by electron microscopy (Fig. 6D). Larazotide acetate also reduced macrophage counts in the lamina propria to control levels (9.5/villi) (Fig. 6C). Macrophage infiltration is one of the earliest responses to gliadin indicating activation of the innate immune system after gluten sensitization [39]. We also tested effects of gliadin in conjunction with AT-1002 in this model. In vivo administration of AT-1002 did not further affect the gliadin-induced barrier abnormalities.

4. Discussion

"Barrier dysfunction" and "intestinal leak" are associated with numerous intestinal and extra-intestinal autoimmune conditions, and barrier function is a new target for drug development, drug delivery, and adjuvant development. In this study, we examined the effects of larazotide acetate, an 8-mer peptide and TJ regulator [10,26], on TJ disruption caused by AT-1002, gliadin, and proinflammatory cytokines.

We have previously shown that AT-1002, a ZOT-derived peptide, disrupts TJs, causes actin cytoskeleton rearrangement,

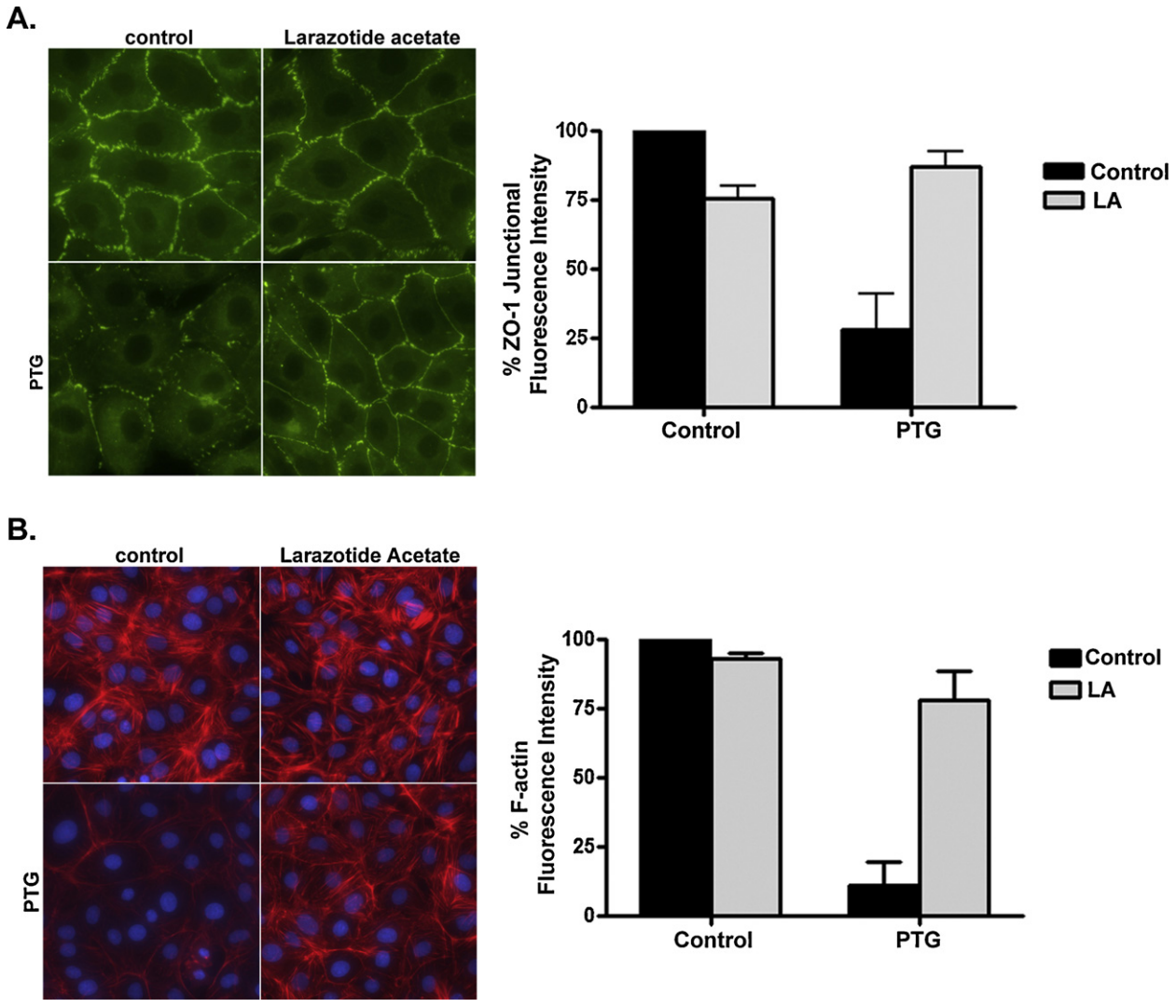

Fig. 3. Larazotide acetate (LA) inhibits PTG-induced ZO-1 redistribution and actin cytoskeletal rearrangement in IEC6 cells. IEC6 cells were treated with PTG (2.5 mg/mL) in the presence or absence of larazotide acetate (12.5 mM) for 1 h at 37 °C. (A) Cells were fixed and processed for immunofluorescence using anti-ZO-1 antibodies. Projections from z-stacks were quantified as described in Section 2. Graph represents percent junctional fluorescence intensity of ZO-1. Data are expressed as mean (SD) and are representative of 2 independent experiments. (B) Cells were fixed, and F-actin was detected using fluorescent phalloidin. Graph represents % F-actin fluorescence intensity. Data are representative of 2 independent experiments.

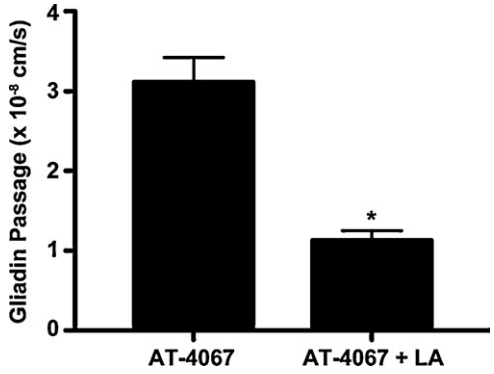

Fig. 4. Larazotide acetate inhibits gliadin translocation across Caco-2 monolayers. Caco-2 cells were treated with FITC-labeled 13-mer gliadin fragment (AT-4067; 1 mM) in the presence or absence of larazotide acetate (LA; 100 μM) for 3 h at 37 °C. At $t = 3$ h, samples were removed from the receiver compartment and analyzed in a fluorescence plate reader at excitation and emission wavelengths of 485 nm and 535 nm, respectively. This gliadin passage was calculated for each treatment and expressed relative to untreated control conditions. Data are expressed as mean (SE) and are representative of 2 independent experiments (3 wells per group per experiment). $^{*}p < 0.05$ vs. control.

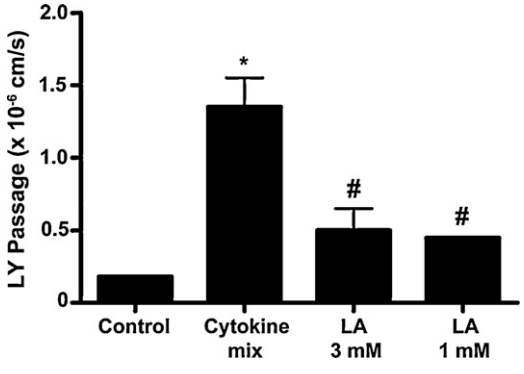

Fig. 5. Larazotide acetate inhibits cytokine-induced tight junction permeability in Caco-2 cells. (A) Caco-2 cells were treated with a mixture of TNF-α, IFNγ, and IL-1β for 72 h. For larazotide acetate treatment, the medium was replaced with different doses of larazotide acetate on the apical side after 48 h. At the end of the experiment, LY passage was measured. Data are expressed as mean (SE) and are representative of 3 independent experiments (3 wells per group per experiment). $^{*}p < 0.05$ vs. control; $^{\#}p < 0.05$ vs. cytokine treatment.

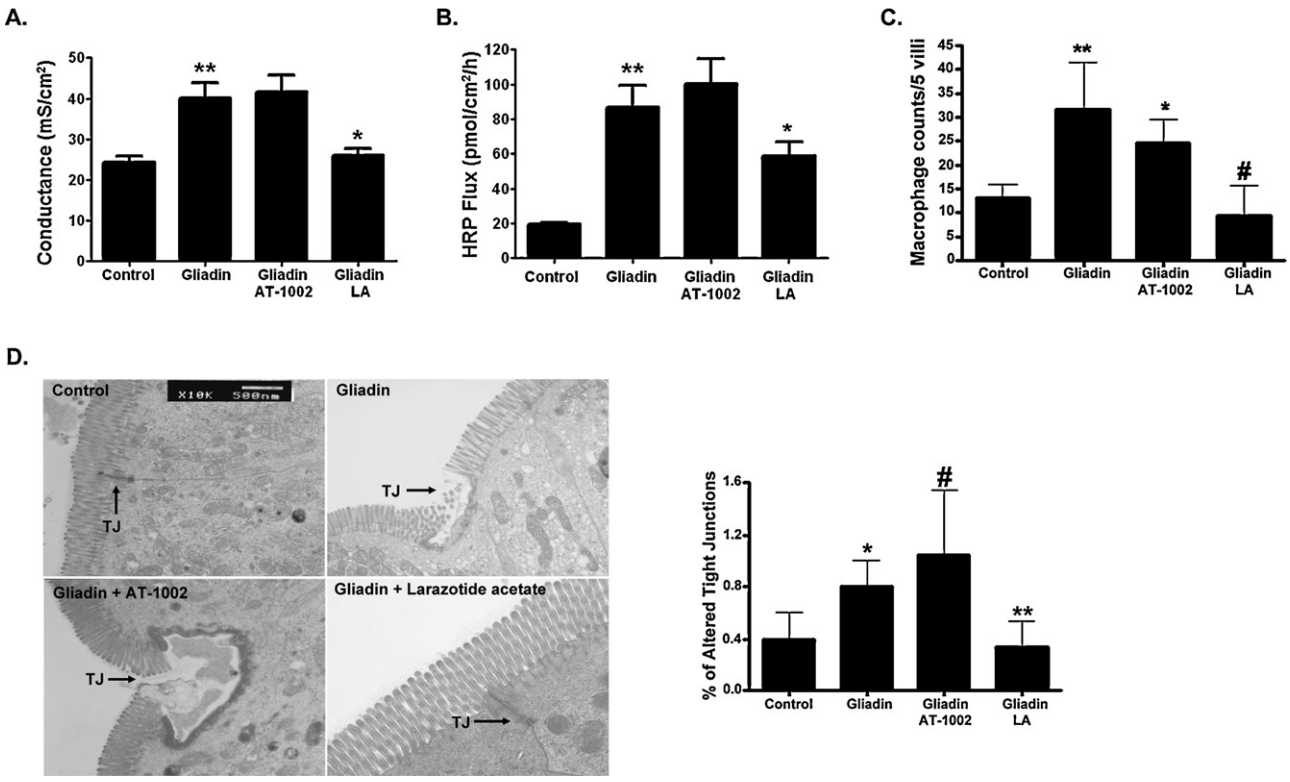

Fig. 6. Larazotide acetate inhibits intestinal permeability in gluten-sensitive transgenic mice. Cohorts of HLA-HCD4/DQ8 mice ($n = 10$ each) were sensitized (i.p.) with gliadin (500 μg) and Complete Freund's Adjuvant (CFA), and thereafter were gavaged with gliadin (2 mg/mouse), +/− treatment, 2×/week for 7 weeks. Group 1 received larazotide acetate (LA; 250 μg/mouse) and gliadin, Group 2 received AT-1002 (250 μg/mouse) and gliadin, and Group 3 was gavaged with gliadin only. A group of non-sensitized controls (CFA; i.p. only) was gavaged with rice. At 24 h after the last gavage, small intestinal tissue was mounted in Ussing chambers for the measurement of following parameters: (A) conductance and (B) permeability (horseradish peroxidase [HRP] flux). (C) Tissue was obtained for the examination of macrophage counts by immunohistochemistry (F4/80) ($^{*}p < 0.01$ vs. gliadin; $^{**}p < 0.01$ vs. control; $^{\#}p < 0.05$ vs. gliadin + AT-1002. (D) Electron micrographs and quantitation showing the preservation of TJ structures by larazotide acetate ($^{*}p < 0.05$ vs. control; $^{\#}p < 0.01$ vs. control; $^{**}p < 0.01$ vs. gliadin). Data are expressed as mean (SD).

phosphorylation and redistribution of ZO-1, and activates src and MAP kinase pathways in vitro [19]. AT-1002 also enhances the systemic exposure of antigens, such as salmon calcitonin, in vivo [38]. In the present study, AT-1002 increased paracellular permeability and elicited actin rearrangement and ZO-1 redistribution in Caco-2 cells, as shown previously [19]. Larazotide acetate inhibited the AT-1002-induced increase in permeability, and this correlated with its ability to inhibit AT-1002-induced actin and ZO-1 redistribution.

In celiac disease, barrier function is compromised and celiac disease patients exhibit enhanced intestinal permeability and disrupted TJs [24,34]. Barrier function is regulated by TJ proteins and the actin cytoskeleton. Agents that disrupt the actin cytoskeleton affect paracellular permeability [21,41]. In our study, PTG caused actin network disassembly, which was inhibited by larazotide acetate. This result is consistent with that of Clemente et al. who showed that larazotide acetate inhibits gliadin-induced cytoskeletal reorganization in IEC-6 cells [9]. PTG has also been shown to induce ZO-1 and occludin redistribution in an in vitro three-dimensional model system and intestinal epithelial cells [11,30]. In accordance with these observations, PTG induced ZO-1 redistribution in IEC-6 cells, which was inhibited by larazotide acetate.

In celiac disease, the mechanisms underlying gliadin peptide transport from the gut lumen to the lamina propria are not well understood. No agreement has been reached in the literature about whether the initial mode of gliadin transport is transcellular, paracellular, or both. Secretory IgA has been shown to mediate intestinal transport of gliadin 33-mer and 19-mer peptides via the CD71 transferrin receptor [23]. In the present study, labeled gliadin peptides translocated from the apical to the basolateral side of a fully differentiated Caco-2 monolayer. Larazotide acetate inhibited the transport of FITC-labeled gliadin 13-mer peptide by more than 50%. Compromised barrier function may allow gliadin to cross the paracellular space. We have also presented convincing evidence that larazotide acetate is an inhibitor of paracellular permeability, which is consistent with recent findings by Silva et al. [37]. However, crosstalk and interaction between the paracellular and transcellular pathways have been demonstrated [43]. Thus, larazotide acetate may inhibit the transport of gliadin peptide regardless of the transport route.

Gliadin peptides cause immune activation and initiate a cascade of inflammatory cytokines, which have been shown to enhance the permeability of the gut epithelium [2,8]. The enhanced permeability would allow more gliadin peptides to enter the lamina propria, which in turn would lead to an increase in inflammatory cytokine levels, and an "inflammatory-permeability loop" would be established. A novel way to treat celiac disease would be to break the inflammatory-permeability loop. Here, we show that larazotide acetate can break the proposed inflammatory-permeability loop by decreasing the transport of inflammatory gliadin peptides, and by inhibiting the increased permeability induced by cytokines.

Interestingly, larazotide acetate inhibited transport of gliadin peptides even at 0.1 mM, which is 100-fold lower than that required to inhibit the AT-1002-induced effects. It is known that in animal experiments using BB Wor rats [46] and IL-10 −/− mice [3], the effective in vivo dose of larazotide acetate is on the order of 0.2–100 μM. In this study, a single dose of larazotide acetate at approximately 100 μM was found to be active in a gluten sensitivity model. However, the concentration of larazotide acetate required to effectively inhibit the effect of cytokines, gliadin peptides, or

AT-1002 in vitro varied considerably (from 0.1 to 10 mM). The reasons for this discrepancy are not known.

We have previously found that intraperitoneal sensitization with gliadin and CFA, followed by an oral gliadin challenge to single transgenic HLA-DQ8 mice increases neurally stimulated ion transport [44]. We have also shown that gliadin sensitization of HLA-HCD4-DQ8 mice increases paracellular and transcellular permeability of macromolecules as assessed by ^{51}Cr-EDTA and HRP flux, respectively [28,37]. In this study we found increased conductance values in gliadin-sensitized mice, indicating a reduction in tissue resistance and suggesting an alteration in the paracellular pathway. This change was normalized by larazotide acetate therapy. This is in agreement with the recent finding of Silva et al. that larazotide acetate also normalizes paracellular macromolecule transport [37]. We also showed that increased HRP flux, indicative of transcellular permeability, was improved with larazotide acetate, but values were still high compared to non-sensitized controls. Improvement in HRP flux by larazotide acetate may relate to overall enhancement of epithelial homeostasis, as it correlated with an improvement in TJ structure in EM and a decrease in macrophage infiltration in gliadin-sensitized and challenged mice. We expected that AT-1002, a permeability enhancing peptide, would augment gliadin's detrimental effects in the intestine. In fact, in a recent study AT-1002 was shown to increase intestinal permeability in vivo [3]. In this study however, AT-1002 did not augment the effect of gliadin in any of the measures. Perhaps AT-1002 cannot add to the already extensive effects of gliadin.

Taken together, our data indicate that larazotide acetate inhibits the cytoskeletal rearrangement and ZO-1 redistribution caused by gliadin and AT-1002 in epithelial cells. Larazotide acetate inhibits gliadin transport in vitro and preserves barrier function in vitro and in vivo. Furthermore, in an in vivo gluten sensitivity model, larazotide acetate inhibited gliadin-induced macrophage accumulation in the intestine and preserved normal TJ structure. These data offer insights into larazotide acetate's mechanisms of action for the treatment of gluten-induced enteropathy, and provide support for larazotide acetate as a novel candidate with potential therapeutic value in the management of celiac disease.

Acknowledgments

This work was partially supported by grants from the Canadian Association of Gastroenterology (CAG)/Canadian Institute of Health Research (CIHR) (GN2-114709), the Canadian Celiac Association New Investigator Award (to E. Verdu), and ALBA Therapeutics. E. Verdu holds a McMaster University Dep. of Medicine Internal Career Research Award. Joseph Murray was supported by NIH grant DK 70031. We are grateful to Drs. Alessio Fasano, Linda Arterburn, and Francisco Leon for critical reading of the manuscript.

References

[1] Aijaz S, Balda MS, Matter K. Tight junctions: molecular architecture and function. Int Rev Cytol 2006;248:261–98.
[2] Al-Sadi R, Ye D, Dokladny K, Ma TY. Mechanism of IL-1beta-induced increase in intestinal epithelial tight junction permeability. J Immunol 2008;180:5653–61.
[3] Arrieta MC, Bistritz L, Meddings JB. Alterations in intestinal permeability. Gut 2006;55:1512–20.
[4] Artursson P, Magnusson C. Epithelial transport of drugs in cell culture. II: Effect of extracellular calcium concentration on the paracellular transport of drugs of different lipophilicities across monolayers of intestinal epithelial (Caco-2) cells. J Pharm Sci 1990;79:595–600.
[5] Black KE, Murray JA, David CS. HLA-DQ determines the response to exogenous wheat proteins: a model of gluten sensitivity in transgenic knockout mice. J Immunol 2002;169:5595–600.
[6] Bodinier M, Legoux MA, Pineau F, Triballeau S, Segain JP, Brossard C, et al. Intestinal translocation capabilities of wheat allergens using the Caco-2 cell line. J Agric Food Chem 2007;55:4576–83.
[7] Ciccocioppo R, Finamore A, Ara C, Di Sabatino A, Mengheri E, Corazza GR. Altered expression, localization, and phosphorylation of epithelial junctional proteins in celiac disease. Am J Clin Pathol 2006;125:502–11.
[8] Clayburgh DR, Shen L, Turner JR. A porous defense: the leaky epithelial barrier in intestinal disease. Lab Invest 2004;84:282–91.
[9] Clemente MG, De Virgiliis S, Kang JS, Macatagney R, Musu MP, Di Pierro MR, et al. Early effects of gliadin on enterocyte intracellular signalling involved in intestinal barrier function. Gut 2003;52:218–23.
[10] Crespo Perez L, Castillejo de Villasante G, Cano Ruiz A, Leon F. Non-dietary therapeutic clinical trials in coeliac disease. Eur J Intern Med 2012;23:9–14.
[11] Dolfini E, Roncoroni L, Elli L, Fumagalli C, Colombo R, Ramponi S, et al. Cytoskeleton reorganization and ultrastructural damage induced by gliadin in a three-dimensional in vitro model. World J Gastroenterol 2005;11:7597–601.
[12] Elli L, Roncoroni L, Doneda L, Ciulla MM, Colombo R, Braidotti P, et al. Imaging analysis of the gliadin direct effect on tight junctions in an in vitro three-dimensional Lovo cell line culture system. Toxicol In Vitro 2011;25:45–50.
[13] Ellis HJ, Rosen-Bronson S, O'Reilly N, Ciclitira PJ. Measurement of gluten using a monoclonal antibody to a coeliac toxic peptide of A-gliadin. Gut 1998;43:190–5.
[14] Fasano A, Shea-Donohue T. Mechanisms of disease: the role of intestinal barrier function in the pathogenesis of gastrointestinal autoimmune diseases. Nat Clin Pract Gastroenterol Hepatol 2005;2:416–22.
[15] Fink MP, Delude RL. Epithelial barrier dysfunction: a unifying theme to explain the pathogenesis of multiple organ dysfunction at the cellular level. Crit Care Clin 2005;21:177–96.
[16] Furuse M. Molecular basis of the core structure of tight junctions. Cold Spring Harb Perspect Biol 2010;2:a002907.
[17] Garrote JA, Gomez-Gonzalez E, Bernardo D, Arranz E, Chirdo F. Celiac disease pathogenesis: the proinflammatory cytokine network. J Pediatr Gastroenterol Nutr 2008;47(Suppl. 1):S27–32.
[18] Ginski MJ, Taneja R, Polli JE. Prediction of dissolution-absorption relationships from a continuous dissolution/Caco-2 system. AAPS Pharm Sci 1999;1:E3.
[19] Gopalakrishnan S, Pandey N, Tamiz AP, Vere J, Carrasco R, Somerville R, et al. Mechanism of action of ZOT-derived peptide AT-1002, a tight junction regulator and absorption enhancer. Int J Pharm 2009;365:121–30.
[20] Kagnoff MF. Celiac disease: pathogenesis of a model immunogenetic disease. J Clin Invest 2007;117:41–9.
[21] Madara JL, Barenberg D, Carlson S. Effects of cytochalasin D on occluding junctions of intestinal absorptive cells: further evidence that the cytoskeleton may influence paracellular permeability and junctional charge selectivity. J Cell Biol 1986;102:2125–36.
[22] Marinaro M, Fasano A, De Magistris MT. Zonula occludens toxin acts as an adjuvant through different mucosal routes and induces protective immune responses. Infect Immun 2003;71:1897–902.
[23] Matysiak-Budnik T, Moura IC, Arcos-Fajardo M, Lebreton C, Menard S, Candalh C, et al. Secretory IgA mediates retrotranscytosis of intact gliadin peptides via the transferrin receptor in celiac disease. J Exp Med 2008;205:143–54.
[24] Montalto M, Cuoco L, Ricci R, Maggiano N, Vecchio FM, Gasbarrini G. Immunohistochemical analysis of ZO-1 in the duodenal mucosa of patients with untreated and treated celiac disease. Digestion 2002;65:227–33.
[25] Natividad JM, Huang X, Slack E, Jury J, Sanz Y, David C, et al. Host responses to intestinal microbial antigens in gluten-sensitive mice. PLoS One 2009;4:e6472.
[26] Paterson BM, Lammers KM, Arrieta MC, Fasano A, Meddings JB. The safety, tolerance, pharmacokinetic and pharmacodynamic effects of single doses of AT-1001 in coeliac disease subjects: a proof of concept study. Aliment Pharmacol Ther 2007;26:757–66.
[27] Picarelli A, Di Tola M, Sabbatella L, Anania MC, Di Cello T, Greco R, et al. 31–43 amino acid sequence of the alpha-gliadin induces anti-endomysial antibody production during in vitro challenge. Scand J Gastroenterol 1999;34:1099–102.
[28] Pinier M, Verdu EF, Nasser-Eddine M, David CS, Vezina A, Rivard N, et al. Polymeric binders suppress gliadin-induced toxicity in the intestinal epithelium. Gastroenterology 2009;136:288–98.
[29] Rubio-Tapia A, Murray JA. Celiac disease. Curr Opin Gastroenterol 2010;26:116–22.
[30] Sander GR, Cummins AG, Henshall T, Powell BC. Rapid disruption of intestinal barrier function by gliadin involves altered expression of apical junctional proteins. FEBS Lett 2005;579:4851–5.
[31] Sawada N, Murata M, Kikuchi K, Osanai M, Tobioka H, Kojima T, et al. Tight junctions and human diseases. Med Electron Microsc 2003;36:147–56.
[32] Schmitz H, Fromm M, Bentzel CJ, Scholz P, Detjen K, Mankertz J, et al. Tumor necrosis factor-alpha (TNFalpha) regulates the epithelial barrier in the human intestinal cell line HT-29/B6. J Cell Sci 1999;112(Pt 1):137–46.
[33] Schneeberger EE, Lynch RD. The tight junction: a multifunctional complex. Am J Physiol Cell Physiol 2004;286:C1213–28.
[34] Schulzke JD, Bentzel CJ, Schulzke I, Riecken EO, Fromm M. Epithelial tight junction structure in the jejunum of children with acute and treated celiac sprue. Pediatr Res 1998;43:435–41.
[35] Schumann M, Richter JF, Wedell I, Moos V, Zimmermann-Kordmann M, Schneider T, et al. Mechanisms of epithelial translocation of the alpha(2)-gliadin-33mer in coeliac sprue. Gut 2008;57:747–54.
[36] Shan L, Molberg O, Parrot I, Hausch F, Filiz F, Gray GM, et al. Structural basis for gluten intolerance in celiac sprue. Science 2002;297:2275–9.
[37] Silva MA, Jury J, Sanz Y, Wiepjes M, Huang X, Murray JA, et al. Increased bacterial translocation in gluten-sensitive mice is independent of small intestinal paracellular permeability defect. Dig Dis Sci 2012.

[38] Song KH, Fasano A, Eddington ND. Enhanced nasal absorption of hydrophilic markers after dosing with AT1002, a tight junction modulator. Eur J Pharm Biopharm 2008;69:231–7.
[39] Thomas KE, Sapone A, Fasano A, Vogel SN. Gliadin stimulation of murine macrophage inflammatory gene expression and intestinal permeability are MyD88-dependent: role of the innate immune response in Celiac disease. J Immunol 2006;176:2512–21.
[40] Tsukita S, Furuse M, Itoh M. Multifunctional strands in tight junctions. Nat Rev Mol Cell Biol 2001;2:285–93.
[41] Turner JR, Rill BK, Carlson SL, Carnes D, Kerner R, Mrsny RJ, et al. Physiological regulation of epithelial tight junctions is associated with myosin light-chain phosphorylation. Am J Physiol 1997;273:C1378–85.
[42] Ukabam SO, Clamp JR, Cooper BT. Abnormal small intestinal permeability to sugars in patients with Crohn's disease of the terminal ileum and colon. Digestion 1983;27:70–4.
[43] Van Driessche W, Kreindler JL, Malik AB, Margulies S, Lewis SA, Kim KJ. Interrelations/cross talk between transcellular transport function and paracellular tight junctional properties in lung epithelial and endothelial barriers. Am J Physiol Lung Cell Mol Physiol 2007;293:L520–4.
[44] Verdu EF, Huang X, Natividad J, Lu J, Blennerhassett PA, David CS, et al. Gliadin-dependent neuromuscular and epithelial secretory responses in gluten-sensitive HLA-DQ8 transgenic mice. Am J Physiol Gastrointest Liver Physiol 2008;294:G217–25.
[45] Wang F, Schwarz BT, Graham WV, Wang Y, Su L, Clayburgh DR, et al. IFN-gamma-induced TNFR2 expression is required for TNF-dependent intestinal epithelial barrier dysfunction. Gastroenterology 2006;131:1153–63.
[46] Watts T, Berti I, Sapone A, Gerarduzzi T, Not T, Zielke R, et al. Role of the intestinal tight junction modulator zonulin in the pathogenesis of type I diabetes in BB diabetic-prone rats. Proc Natl Acad Sci U S A 2005;102:2916–21.